

Star formation in outer rings of S0 galaxies. V.

UGC 4599 – an S0 with gas probably accreted from a filament.

O. Sil'chenko¹, A. Moiseev^{2,1}, D. Oparin², J. E. Beckman^{3,4}, and J. Font^{3,4,5}

¹ Sternberg Astronomical Institute of the Lomonosov Moscow State University, University av. 13, 119234 Russia
e-mail: olga@sai.msu.su

² Special Astrophysical Observatory of the Russian Academy of Sciences, Nizhnij Arkhyz, 369167 Russia
e-mail: moisav@gmail.com, doparin@mail.ru

³ Instituto de Astrofísica de Canarias, 38205 La Laguna, Tenerife, Spain

⁴ Departamento de Astrofísica, Universidad de La Laguna, Tenerife, Spain

⁵ Observatorio Gemini Sur, NOIRLAB, La Serena, Chile

Received ..., 2022; accepted ..., 2022

ABSTRACT

Aims. Though S0 galaxies are usually thought to be ‘red and dead’, they often demonstrate weak star formation organised in ring structures and located in their outer disks. We try to clarify the nature of this phenomenon and its difference from star formation in spiral galaxies. The moderate-luminosity nearby S0 galaxy, UGC 4599, is studied here.

Methods. By applying long-slit spectroscopy at the Russian 6m telescope, we have measured stellar kinematics for the main body of the galaxy and strong emission-line flux ratios in the ring. After inspecting the gas excitation in the ring using line ratio diagrams and having shown that it is ionised by young stars, we have determined the gas oxygen abundance by using conventional strong-line calibration methods. We have inspected the gas kinematics in the ring with Fabry-Perot interferometre data obtained at the William Herschel Telescope. The pattern and properties of the brightest star formation regions are studied with the tunable filter MaNGaL at the 2.5m telescope of the Caucasian Mountain Observatory of the Sternberg Astronomical Institute (CMO SAI MSU).

Results. The gas metallicity in the ring is certainly subsolar, $[O/H] = -0.4 \pm 0.1$ dex, that is different from the majority of the outer starforming rings in S0s studied by us which have typically nearly solar metallicity. The total stellar component of the galaxy which is old in the center is less massive than its extended gaseous disk. We conclude that probably the ring and the outer disk of UGC 4599 are a result of gas accretion from a cosmological filament.

Key words. galaxies: structure – galaxies: evolution – galaxies, elliptical and lenticular – galaxies: star formation

1. Introduction

The morphological type S0 was initially introduced as star-formation free disk galaxies (Hubble 1936), while outer rings were early recognised as common attributes of S0 galaxies (de Vaucouleurs 1959). Later a significant amount of cold gas has been found in many S0 galaxies, and in half of gas-rich S0s the gas feeds star formation organised in ring structures (Pogge & Eskridge 1993). Moreover more than the half of outer stellar rings in S0s are bright in ultraviolet (UV) so betraying recent star formation on a timescale of a few hundred Myr (Kostiuk & Sil'chenko 2015). In the frame of the current paradigm according to which evolution of disk galaxies is driven by persistent accretion of outer cold gas, this situation with S0s is quite understandable because in sparse environments the S0s may suffer the same outer gas accretion as spirals, with a possibility of star formation in accreted gas. However, the source of outer gas accretion remains still unknown. Cosmologists are sure that this source is provided by large-scale Universe structure, in particular, by large-scale filaments filled by dark matter and primordial gas (Ocvirk et al. 2008, e.g.). The observations reveal nearly solar metallicity in the outer starforming rings of S0 galaxies favouring rather gas-rich satellite merging (Sil'chenko et al. 2019; Sil'chenko & Moiseev 2020). In this Letter we examine an outer starforming ring in UGC 4599, a

moderate-luminosity nearby S0 galaxy, which has indeed rather low metallicity and can therefore be fed by primordial gas from cosmological filaments.

The galaxy image taken from the LegacySurvey resource (Dey et al. 2019) including the data from the DECaLS photometric survey is presented in Fig. 1. It is seen almost face-on, and with the adopted distance of 32 Mpc (cosmology-corrected luminosity distance from the NASA Extragalactic Database, NED) the radius of the ring is 7.7 kpc. Finkelman & Brosch (2011) claimed that UGC 4599 is an analog of the famous Hoag galaxy, so being a small elliptical surrounded by a detached ring. However there were also other opinions: Dowell (2010) treated UGC 4599 as a classical S0, with the de-Vaucouleurs' bulge contributing only 32% to the total luminosity, and a low-surface-brightness (LSB) exponential disk. Gutiérrez et al. (2011) found even more disks: they classified UGC 4599 as a Type-III-d so discovering *two* LSB disks, with the exponential scalelengths of 6.5 kpc and 10 kpc. Indeed, the deep image in Fig. 1 allows us to trace the UGC 4599 blue disk extending well beyond the ring radius. The galaxy is extremely rich in HI: the data of the ALFALFA survey reveal about $10^{10} M_{\odot}$ of neutral hydrogen, with the diameter of the HI disk of ~ 100 kpc (Grossi et al. 2009). We have undertaken further investigation of the galaxy by applying long-slit spectroscopy, Fabry-Perot interferometry, and narrow-band imaging in the strong emission lines.

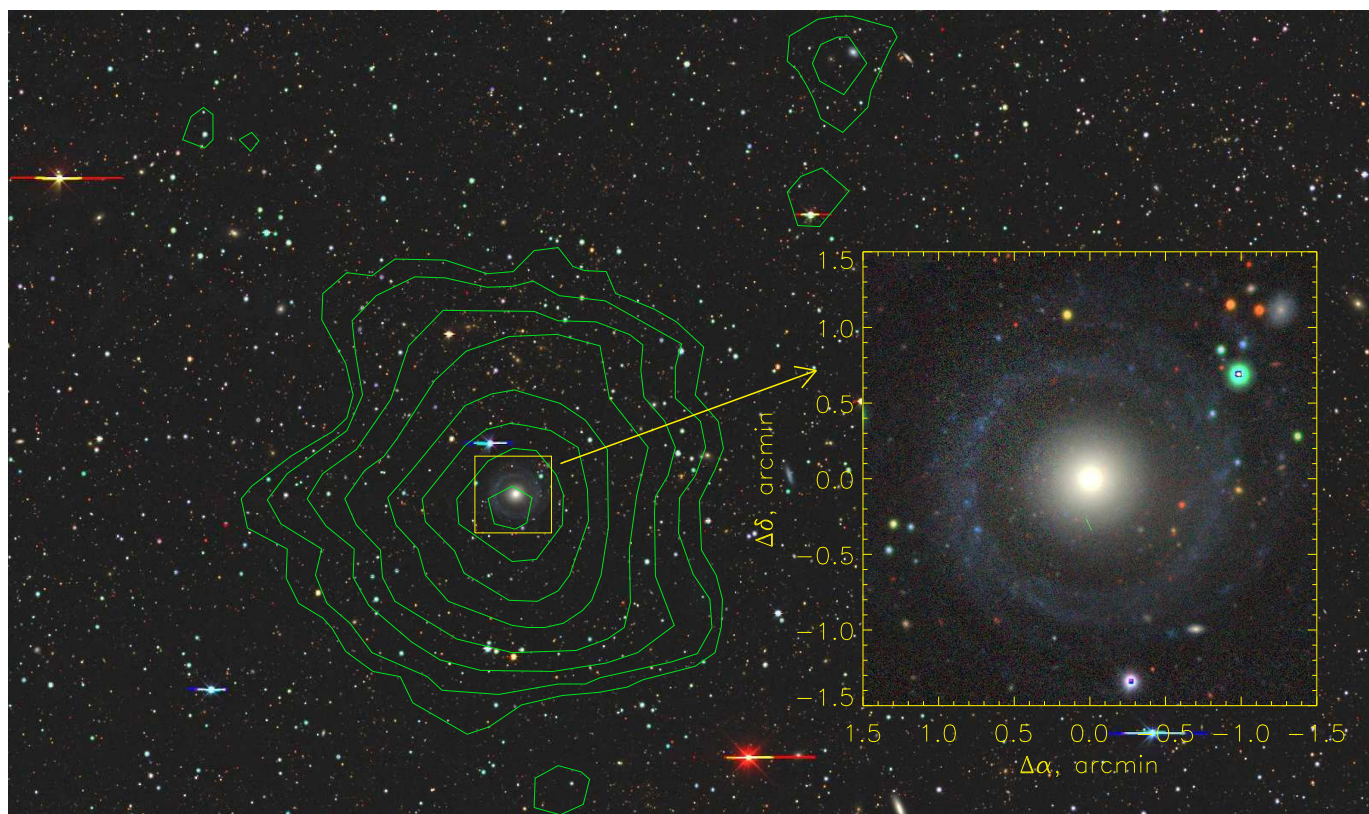


Fig. 1. The Legacy Imaging Surveys colour image of the UGC 4599 and its environments. The HI density contours are overlaid following Grossi et al. (2009). The north is up, the east is to the left.

2. Observations and the data involved

Our long-slit spectral observations were made with a multi-mode reducer SCORPIO-2 (Afanasiev & Moiseev 2011) at the prime focus of the Russian 6m telescope of the Special Astrophysical Observatory, Russian Academy of Sciences (SAO RAS). UGC 4599 was observed on February 25th, 2014, at $PA(\text{slit}) = 115^\circ$, with the total exposure time of 75 min, on March 26th, 2015, in the orientation through the neighbouring galaxy (designated by *A* in Fig. 2, the third plot), at $PA(\text{slit}) = 132^\circ$, with the total exposure time of 60 min, and with a short exposure at $PA(\text{slit}) = 49^\circ$ in February 2022. The slit orientations are shown in Fig. 2. During the observations the range of airmass was 1.2–1.5. The seeing was $\sim 1''$, the VPHG1200 grism provided an intermediate spectral resolution FWHM $\approx 5 \text{ \AA}$ in the wavelength region from 4000 \AA to 7200 \AA . This spectral range includes a set of strong absorption and emission lines making it suitable to analyse both stellar and gaseous kinematics of the galaxy as well as the gas excitation and chemistry. The slit is $1''$ in width and $6'$ in length allowing us to use the edge spectra to subtract the sky background. The CCD E2V 42-90, with a format of 2048×4600 , used in the 1×2 binning mode provided a spatial scale of $0.357''$ per px and a spectral sampling of $0.86 \text{ \AA}/\text{px}$. The data reduction as well as the derivation of the characteristics of the gaseous kinematics were standard for our SCORPIO-2 data – see for example Proshina et al. (2020). The profiles of the line-of-sight stellar velocity have been calculated by cross-correlation of galactic spectra binned along the slit with the best-matched template spectra of K-type stars from the library MILES (Sánchez-Blázquez et al. 2006).

To study the kinematics in the $H\alpha$ emission we obtained the data using the Fabry-Perot Interferometer GH α FaS

(Hernandez et al. 2008) on the William Herschel Telescope (WHT) at the Roque de los Muchachos Observatory, La Palma. GH α FaS has a circular field of view of 3.4 arcmin, free spectral range of 8 \AA which corresponds to 390 km s^{-1} with a velocity resolution of 8 km s^{-1} , with spatial sampling of $0.2''$. The observations were undertaken on March 14th, 2016, with the total exposure of 160 s in each of 40 spectral channels. The seeing was $1.2''$.

We also carried out observations at the 2.5m CMO SAI MSU telescope with a narrow-band tuned photometer MaNGaL (Moiseev et al. 2020). The observations were performed in two redshifted emission lines, [OIII] $\lambda 5007$ and [NII] $\lambda 6583$, within the band of 13 \AA , to study the surface brightness distributions in these lines characterising the ionised gas in the ring. The detector, CCD iKon-M934 with the format of 1024×1024 , provided the field of view of 5.4 arcmin and the sampling of $0.33''$ per pixel. The observations were undertaken on November 14th, 2020, for [NII] $\lambda 6583$, with an exposure time of 75 min, and on November 17th, 2020, for [OIII] $\lambda 5007$, with an exposure time of 60 min. The seeing was $1.3''$ on the first date and $1.9''$ on the second date.

To study the large-scale structure of the galaxy, we have used the *gr*-band images from the LegacySurvey (the DECaLS data).

3. Emission lines in the ring of UGC 4599

The ring of the galaxy at $R \sim 50''$ prominent in the optical continuum (Fig. 1) and in the UV (Fig. 2), is also well traced by the emission-line regions in the [OIII] $\lambda 5007$ line (Fig. 2, left): we can notice more than a dozen compact emission-line sources in the Fig. 2 (left). Only a few of these regions are also seen in the [NII] $\lambda 6583$ emission line (Fig. 2), and these detections

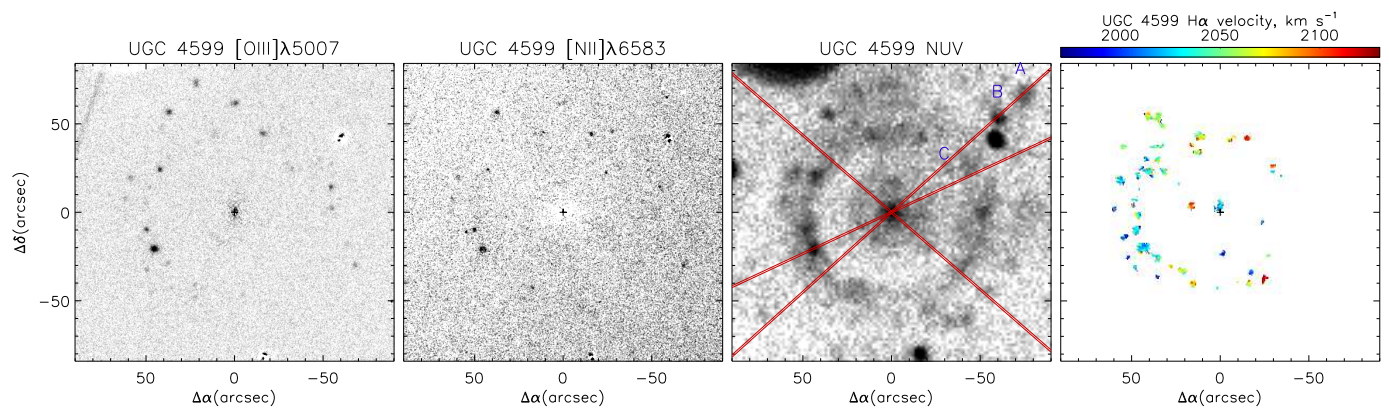


Fig. 2. The MaNGaL images of UGC 4599, from left to right: in the emission line [OIII] λ 5007 and [NII] λ 6583; then the GALEX NUV image with the SCORPIO-2 slit orientations overplotted and the H α velocity field taken with GH α FaS. At every plot, the north is up, the east is to the left.

are mostly concentrated in the eastern half of the ring. This difference in the surface distributions of the high-excitation and low-excitation emission lines is confirmed by the literature data: Dowell (2010) and Finkelman & Brosch (2011) analysed the narrow-band deep images of UGC 4599 in H α obtained within the spectral windows including both H α and [NII] λ 6583 and also noted only HII-regions concentrated in the eastern and northern part of the ring. Salzer et al. (2020) searched for compact star-forming galaxies by using deep narrow-band photometry in the H α line and found four HII-regions in the ring of UGC 4599 (their no.103, 104, 105, 106); for these 'HaDots' the full-range spectra were also obtained at the Hobby-Eberly 9.2m telescope (HET). We use their emission-line ratios together with our results to inspect the gas excitation (Fig. 3).

Our long slit at $PA(\text{slit}) = 115^\circ$ crossed the eastern emission-line region, the brightest one in the ring, and our long slit at $PA(\text{slit}) = 132^\circ$ passed through a small galaxy to the north-west from UGC 4599 which is designated by 'A' in Fig. 2. In fact, when we looked at the spectrum we saw a lot of emission-line objects to the north-west from the centre of UGC 4599 (Fig.3). Two of them belong to the ring of the galaxy which is split into two arms to the west; and three of them are background galaxies with redshifts of 0.08 (A), 0.360 (B), and 0.324 (C).

We use the strong emission-line flux ratios to check the gas excitation by inspecting the so called Baldwin-Phillips-Terlevich(BPT)-diagram (Baldwin et al. 1981) in Fig. 3. All the HII-regions with full-range spectra – four in the eastern part of the ring measured by Salzer et al. (2020) and our data for the brightest eastern region, and two our cross-sections of the ring to the north-west from the centre – indeed show HII-type excitation, as they are located to the left of the dividing lines prescribed by Kewley et al. (2001) and Kauffmann et al. (2003). Then we can determine the ionised-gas oxygen abundance by using the strong-line calibrations. We have involved the widely used calibrations from Perez-Montero (2014) and Marino et al. (2013). By averaging the oxygen abundances derived from our measurements of N2 and O3N2 for three more bright HII-regions, we have obtained $12 + \log(\text{O}/\text{H}) = 8.23 \pm 0.05$ dex from the Marino et al. (2013) calibrations. The models by Perez-Montero (2014) involving the measurements of 6 emission lines, H β , [OIII] λ 5007, H α , [NII] λ 6583, [SII] λ 6717,6731, give $12 + \log(\text{O}/\text{H}) = 8.40 \pm 0.11$ dex.

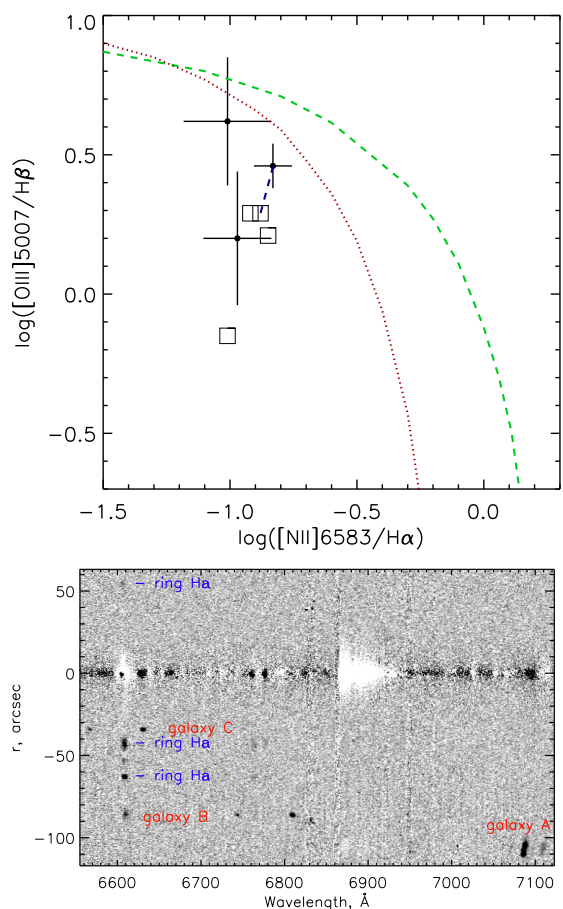


Fig. 3. The emission lines in the ring of UGC 4599 and nearby galaxies. In the upper plot – the BPT-diagram for the ring HII-regions, both from our long-slit spectroscopy (with error bars) and from Salzer et al. (2020) (squares). The measurements for the common HII-region are connected by a blue dashed line. The excitation-mechanism dividing lines are from Kewley et al. (2001) (the green dashed line) and from Kauffmann et al. (2003) (the red dotted line). In the bottom plot – the view of the red part of the continuum-subtracted long-slit spectrum at $PA = 132^\circ$.

4. The central stellar spin and the gas kinematics in the ring of UGC 4599

For the main optical emission line of starforming regions, H α , we have observed UGC 4599 with the scanning Fabry-Perot in-

ferometre at the 4.2m WHT to derive not only the $H\alpha$ map, but also the line-of-sight (LOS) velocity map reflecting the projection of the ionised-gas rotation in the ring. The results are presented in Fig. 2, right. Under the assumption of planar circular gas rotation we can restrict the gaseous disk orientation by using the two-dimensional LOS velocity distribution: at a fixed radius the projection of the tangential rotation velocity would be maximal at the line of nodes of the gaseous disk and would be zero in the orthogonal direction. Using the tilted-ring model of circular rotation as described in Sil'chenko et al. (2019) we obtained the orientation of the line of nodes of the gaseous disk at the radius of the ring: $PA_0 = 271^\circ \pm 9^\circ$. As for the inclination, we can estimate it by plotting UGC 4599, with its HI line width $W_{50} = 148 \text{ km s}^{-1}$ (Grossi et al. 2009) and its baryonic mass, stellar plus gaseous, $\log M_b = 10.18$ (Huang et al. 2014), onto the baryonic Tully-Fisher relation from e.g. Lelli et al. (2019), obtaining $i_g \approx 32^\circ$. The orientation of the stellar rotation plane can be estimated from the long-slit data. The photometric inclination of the stellar disk was given by Gutiérrez et al. (2011) as $i_* = 24^\circ$, under the assumption for the disk relative thickness of $q_0 = 0.2$. Under the more realistic assumption of the relative typical thickness $q_0 = 0.4$ found by us for lenticular galaxies in sparse environments (Sil'chenko et al. 2020), this estimate transforms into $i_* = 26^\circ$. The model line-of-sight velocity profiles calculated with this assumed inclination for three different stellar-disk line-of-nodes orientations are superposed onto our long-slit measurements in Fig. 4. It can be seen that the line-of-nodes position angle of the gaseous disk, $PA_0 = 271^\circ \pm 9^\circ$, can be excluded for the stellar disk due to zero velocity gradient along the $PA = 49^\circ$. By fitting all three long-slit cross-sections (Fig. 4), the best estimate of the line-of-nodes position angle for the central stellar disk would be $PA_0 = 324^\circ \pm 20^\circ$. Evidently, the plane of the gaseous disk is inclined with respect to the central stellar disk. This configuration is dynamically unstable and gives evidence for recent gas accretion.

5. Discussion

5.1. The structure and morphological type of UGC 4599

Opinions on the luminosity and morphological type of UGC 4599 in the literature show differences. For example, Finkelman & Brosch (2011) treated UGC 4599 as a dwarf *elliptical* galaxy, with $M_g = -17.9$ ($M_B = -17.4$) and a detached 8-kpc ring. However, those researchers who focused on its extended HI disk also noted its large *stellar* disk, and then UGC 4599 was classified as an intermediate-luminosity lenticular galaxy: Grossi et al. (2009) estimated its integrated absolute magnitude as $M_B = -19.07$ and Dowell (2010) – as $M_B = -19.42 \pm 0.02$.

We have inspected the rather deep new *gr*-images of UGC 4599 provided by the DECaLS survey. We present our results of isophote analysis and the azimuthally averaged surface brightness profile of UGC 4599 in Fig. 5. Indeed, we do not see any gap between the central body (including perhaps the exponential pseudobulge) and the ring: the ring in the radius range of $45''$ – $65''$ is superposed onto the extended exponential disk which can be fitted over $R = 35''$ – $100''$ range by a model profile $\mu_r = 23.6 + 1.086R/49.1''$. With respect to the measurements by Gutiérrez et al. (2011), we have obtained slightly larger exponential scalelength for the inner portion of the UGC 4599 disk because we have excluded the ring from our fitting. In any case, with its scalelength of 7.5 kpc and its central surface brightness of $\mu_0(r) = 23.6$ the galaxy can be classified as

an LSB disk galaxy. Moreover, when we estimate the integrated characteristics of the disk in Fig. 5 (right), $M_V = -19.8$ and $r_{eff} = 12.6$ kpc, and compare them with the data in Fig. 12 by Greco et al. (2018) and with the data in Fig. 1 by Saburova et al. (2021), we ascertain that UGC 4599 belongs to the class of *giant* LSB disk galaxies and resembles such objects considered by Saburova et al. (2021) as UGC 1378 or UGC 1382.

5.2. The origin of the gaseous disk in UGC 4599

As was found by Saburova et al. (2021), the most frequent scenario of giant LSB galaxy formation is accretion of high-momentum gas from outside. The second most favoured scenario, coplanar merging of two large spiral galaxies (that was also suggested by Finkelman & Brosch (2011)), can be excluded for UGC 4599 by our data because the low oxygen abundance of the ionised gas in the starforming ring contradicts the typically solar abundance of gas in non-dwarf spiral galaxies (Tremonti et al. 2004; Pilyugin et al. 2004). The outer gas accretion scenario is more suitable also because of the inclined orientation of the gaseous ring spin vector with respect to the collective stellar angular momentum. But what can be a source of the outer gas?

The environment of UGC 4599 is rather sparse though the galaxy has been included into galaxy groups by several catalogues: in USGC 191 by Ramella et al. (2002) and in the compact triplet UZC-CG 79 by Focardi & Kelm (2002). Indeed, the group contains three galaxies of comparable luminosities, UGC 4599, UGC 4590, and UGC 4550. The tightest pair separation, between UGC 4599 and UGC 4590, is 179 kpc, and the third galaxy, UGC 4550, is classified as completely isolated in the 2MIG catalog (Karachentseva et al. 2010). It is important to note that UGC 4590 is devoid of neutral hydrogen though demonstrating a starforming nucleus (Grossi et al. 2009). In the latter paper, the authors proposed a hypothesis of gas flow to UGC 4599 from the nearby dwarf PGC 24666 (CGCG 061-011) because several HI clumps were detected between UGC 4599 and CGCG 061-011. But CGCG 061-011 is a very small galaxy, with a stellar mass of $3 \cdot 10^8 M_\odot$ (Alatalo et al. 2016) and HI mass of $4 \cdot 10^8 M_\odot$ (Haynes et al. 2018); it seems improbable that CGCG 061-011 may provide a two order larger mass of neutral hydrogen for UGC 4599. Moreover, the metallicity of the ionised gas may be higher in the dwarf CGCG 061-011 than in UGC 4599. For the latter we have measured $\log [\text{NII}]\lambda 6583/\text{H}\alpha = -0.95 \pm 0.01$ by averaging our emission-line measurements for five HII-regions (it corresponds to $12 + \log (\text{O}/\text{H}) = 8.23$ dex (Marino et al. 2013)). For CGCG 061-011 we have obtained a long-slit spectrum with the SCORPIO-2 on October 31, 2022. After we have excluded the more metal-rich galaxy core, the remaining $\log [\text{NII}]\lambda 6583/\text{H}\alpha$ profile up to $r = 13''$ has appeared to be flat, and it reveals the mean nitrogen-to-hydrogen line ratio of -0.809 ± 0.005 corresponding to $12 + \log (\text{O}/\text{H}) = 8.30 \pm 0.09$ dex (Marino et al. 2013). So the ionised gas in the starforming ring of UGC 4599 is poorer by oxygen than the gas in the dwarf galaxy CGCG 061-011: it cannot be a donor. The completed merger of a small gas-rich satellite is not a good perspective to explain the large HI disk of UGC 4599 too because of its very large mass of accreted neutral hydrogen, $1.1 \cdot 10^{10} M_\odot$ (Haynes et al. 2018); the total stellar mass of UGC 4599 is less than half of this, $M_* = 4 \cdot 10^9 M_\odot$ (Huang et al. 2014). Therefore we cannot identify a suitable galaxy to play the role of gas donor in the vicinity of UGC 4599.

The metallicity of the ionised gas in the ring of UGC 4599 appears to be unusually low, -0.4 dex. Up to now we have studied a dozen outer starforming rings in lenticular galaxies, and the gas metallicities in these rings are very homogeneous, -0.15 dex independently of the galaxy luminosity or ring radius (Sil'chenko et al. 2019; Proshina et al. 2020). By confronting the high relative mass of HI and the low metallicity of the ionised gas, we reach the conclusion that this is perhaps the first clear case of gas accretion to a ring of S0 galaxy from a cosmological filament. Then the chain of HI clumps in the direction from UGC 4599 to PGC 24666 (Grossi et al. 2009) may trace this filament. A quite similar structure has been observed in 21 cm near the Hoag object which is a recognised case of filamentary gas accretion onto an elliptical galaxy (Brosch et al. 2013).

Acknowledgements. This study is based on the data obtained at the unique scientific facility the Big Telescope Alt-azimuthal SAO RAS and was supported under the Ministry of Science and Higher Education of the Russian Federation grant 075-15-2022-262 (13.MNPMU.21.0003). The renovation of 6m telescope equipment is currently provided within the national project "Science". The work used the public data of the Legacy Surveys (<http://legacysurvey.org>), that consists of three individual and complementary projects: the Dark Energy Camera Legacy Survey (DECaLS; Proposal ID #2014B – 0404; PIs: David Schlegel and Arjun Dey), the Beijing-Arizona Sky Survey (BASS; NOAO Prop. ID #2015A – 0801; PIs: Zhou Xu and Xiaohui Fan), and the Mayall z-band Legacy Survey (MzLS; Prop. ID #2016A – 0453; PI: Arjun Dey). DECaLS, BASS and MzLS together include data obtained, respectively, at the Blanco telescope, Cerro Tololo Inter-American Observatory, NSF's NOIRLab; the Bok telescope, Steward Observatory, University of Arizona; and the Mayall telescope, Kitt Peak National Observatory, NOIRLab. The Legacy Surveys project is honored to be permitted to conduct astronomical research on Iolkam Du'ág (Kitt Peak), a mountain with particular significance to the Tohono O'odham Nation. The NASA GALEX mission data for our Fig. 2 were taken from the Mikulski Archive for Space Telescopes (MAST). The William Herschel Telescope is in the Isaac Newton Group of telescopes, situated at the Roque de los Muchachos Observatory, La Palma, of the Instituto de Astrofísica de Canarias (IAC).

References

- Afanasyev, V. L., Moiseev, A. V. 2011, *Baltic Astronomy*, 20, 363
 Alatalo, K., Cales, S. L., Rich, J. A., et al. 2016, *ApJ Suppl. Ser.*, 224, A18
 Baldwin, J. A., Phillips, M. M., Terlevich, R. 1981, *PASP*, 93, 5
 Brosch, N., Finkelman, I., Oosterloo, T., et al. 2013, *MNRAS*, 435, 475
 de Vaucouleurs, G. 1959, *Handbuch der Physik*, 53, 275
 Dey, A., Schlegel, D. J., Lang, D., et al. 2019, *AJ*, 157, A168
 Dowell, J. D. 2010, Ph. D. Thesis, Univ. of Indiana
 Finkelman, I., Brosch, N. 2011, *MNRAS*, 413, 2621
 Focardi, P., Kelm, B. 2002, *A&A*, 391, 35
 Freeman, K. C. 1970, *ApJ*, 160, 767
 Greco, J. P., Greene, J. E., Strauss, M. A., et al. 2018, *ApJ*, 857, 104
 Grossi, M., di Serego Alighieri, S., Giovanardi, C., et al. 2009, *A&A*, 498, 407
 Gutiérrez, L., Erwin, P., Aladro, R., Beckman, J. E. 2011, *AJ*, 142, A145
 Haynes, M. P., Giovanelli, R., Kent, B. R., et al. 2018, *ApJ*, 861, 49
 Hernandez, O., et al. 2008, *PASP*, 120, 665
 Huang, S., Haynes, M. P., Giovanelli, R., et al. 2014, *ApJ*, 793, 40
 Hubble, E. P., 1936, *The Realm of the Nebulae*. New Haven: Yale Univ. Press
 Karachentseva, V. E., Mitronova, S. N., Melnyk, O. V., Karachentsev, I. D. 2010, *Astrophys. Bull.*, 65, 1
 Kauffmann G., Heckman, T. M., Tremonti, Ch., Brinchmann, J., Charlot, S., et al., 2003, *MNRAS*, 346, 1055
 Kewley, L. J., Dopita, M. A., Sutherland, R. S., Heisler, C. A., Trevena, J., 2001, *ApJ*, 556, 121
 Kostniuk, I. P., Sil'chenko, O. K. 2015, *Astrophys. Bull.*, 70, 280
 Lelli, F., McGaugh, S. S., Schombert, J. M., et al. 2019, *MNRAS*, 484, 3267
 Marino, R. A., Rosales-Ortega, F. F., Sánchez, S. F., et al., 2013, *A&A*, 559, A114
 Moiseev, A., Perepelitsyn, A., and Oparin, D., 2020, *Experimental Astronomy* 50, 199
 Ocvirk, P., Pichon, C., Teyssier, R. 2008, *MNRAS*, 390, 1326
 Perez-Montero, E. 2014, *MNRAS*, 441, 2663
 Pilyugin, L. S., Vilchez, J. M., Contini T. 2004, *A&A*, 425, 849
 Pogge, R. W., Eskridge, P. B., 1993, *AJ*, 106, 1405
 Proshina, I., Sil'chenko, O., Moiseev, A. 2020, *A&A*, 634, A102
 Ramella, M., Geller, M. J., Pisani, A., da Costa, L. N. 2002, *AJ*, 123, 2976

- Saburova, A. S., Chilingarian, I. V., Kasparova, A. V., et al. 2021, *MNRAS*, 503, 830
 Salzer, J. J., Feddersen, J. R., Derloshon, K., et al., 2020, *AJ*, 160, A242
 Sánchez-Blázquez, P., Peletier, R. F., Jiménez-Vicente J., et al., 2006, *MNRAS*, 371, 703
 Sil'chenko, O. K., Moiseev, A. V., Egorov, O. V. 2019, *ApJ Suppl. Ser.*, 244, A6
 Sil'chenko, O. K., Moiseev, A. V. 2020, *A&A*, 638, L10
 Sil'chenko, O. K., Kniazev, A. Yu., Chudakova, E. M. 2020, *AJ*, 160, A95
 Tremonti, Ch. A., Heckman, T. M., Kauffmann, G., et al. 2004, *ApJ*, 613, 898

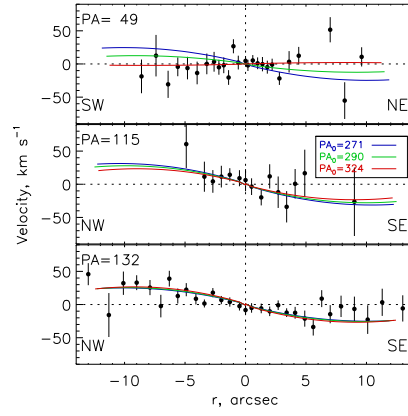


Fig. 4. The line-of-sight velocities of stars along three SCORPIO-2 slit position angles. Coloured lines show the projection of the second-degree polynomial fitting of the mean rotation curve for the various accepted PA_0 .

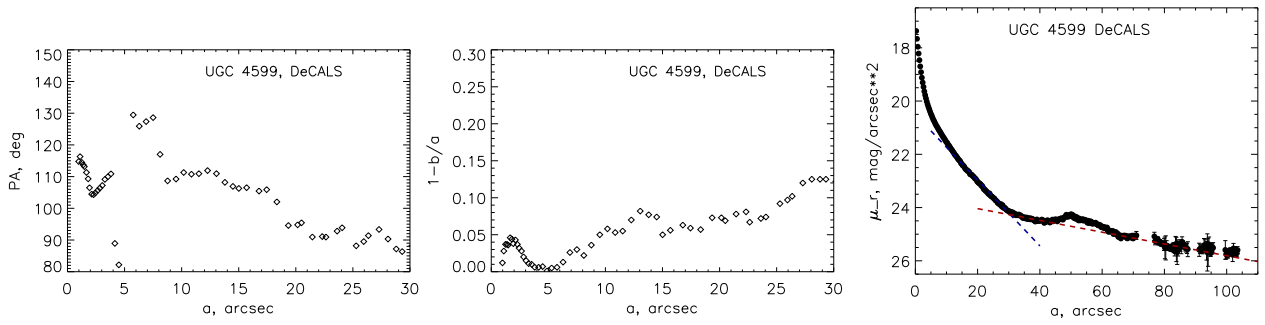


Fig. 5. The results of the analysis of the r -band UGC 4599 image from the DeCaLS survey: isophote characteristics (*the left and central plot*) and the azimuthally averaged surface brightness profile with pseudobulge and inner disk fitted by exponential laws (*the right plot*). The two fitted exponential relations are: $\mu_r = 20.5 + 1.086R/8.8''$ (blue dashed line) and $\mu_r = 23.6 + 1.086R/49.1''$ (red dashed line).